

Article

# High-Temperature Mineral Formation after Firing Clay Materials Associated with Mined Coal in Teruel (Spain)

Manuel Miguel Jordán <sup>1,\*</sup> , Sergio Meseguer <sup>2</sup> , Francisco Pardo <sup>3</sup> and María Adriana Montero <sup>1</sup>

<sup>1</sup> Department of Agrochemistry and Environment (GEA-UMH), University Miguel Hernández, Elche. Avda. de la Universidad s/n, 03202 Elche, Alicante, Spain; adriana@idiomasumh.es

<sup>2</sup> Unit of Applied Mineralogy, Jaume I University, Campus de Riu Sec s/n, 1280 Castellón, Spain; smesegue@camn.uji.es

<sup>3</sup> Department of Education Sciences, CEU Cardenal Herrera University, Calle Grecia 31, 12006 Castellón, Spain; francisco.pardo@uchceu.es

\* Correspondence: manuel.jordan@umh.es; Tel.: +34-966658416

Received: 1 April 2020; Accepted: 28 April 2020; Published: 29 April 2020



**Abstract:** The production of porcelain stoneware has experienced a considerable increase. Therefore, it was necessary to undertake an investigation that would allow knowing the mineralogical evolution that porcelain stoneware undergoes during the firing process, as well as establishing the influence of the formation of mullite and other mineral or vitreous phases and their quantification. The firing transformations of mine spoils associated with mined coal in the Utrillas-Escucha-Estercuel and Ariño-Andorra areas are studied in this paper. The mineralogical composition of the bulk mine spoils is kaolinite, illite, chlorite, and smectites (in traces), with quartz and feldspar, and minor hematite, calcite, and dolomite. The main objective is to understand the generation of high-temperature mineral phases after firing, and their quantification. The formation of mullite and other high-temperature phases are studied from samples that include variable proportions of illite. Samples with a high content of illite generate mullite at 995 °C. Cristobalite was not detected as a high-temperature phase. Mullite is the most abundant mineral. The hercynite content is higher at low temperatures (995 °C), and hematite content is higher at 1150 °C. The vitreous phase represents about 50% of fired bodies. Despite observing a porous microstructure, the non-porous areas are well sintered.

**Keywords:** Teruel; clay spoils; firing transformations; phase generation; vitreous phase; XRD; FTIR

## 1. Introduction

The province of Teruel (NE Spain) has historically been an important coal mining area. In this area there are still abundant coal deposits, but coal mining has ceased in recent decades. In this paper, firing transformations [1] of mine spoils from the mined coal in the Utrillas-Escucha-Estercuel and Ariño-Andorra regions are studied (Figure 1). The production of porcelain stoneware has experienced a considerable increase since its initial development in Italy in the late 1970s [2]. The valuation of these mine spoils can bring economic and environmental benefits [3]. However, this increase in manufacture was not accompanied by the necessary research to know the scope of the reactions that take place during the firing process of the ceramic pieces. It is worth noting the fact that the few publications that exist on the porcelain stoneware microstructure refer, above all, to issues of porosity and glass formation, without addressing the study of mullite formation and mineral quantification [1,2]. Therefore, it was considered necessary to undertake an investigation that would allow knowing the mineralogical and microstructural evolution that porcelain stoneware undergoes during its firing process, as well as establishing the influence of the mullite crystalline phase formation on some

properties as open porosity [2]. For production of porcelain stoneware, ball clays are required [2]. In the Spanish ceramic cluster, white ceramic clays have usually been imported from Ukraine, France, and the UK [3]. However, a greater knowledge of the mine spoils from the lignite mines in Teruel will allow their incorporation as new raw materials in the main ceramic companies [4–6]. The future use of these spoils will represent significant savings in production costs [3].

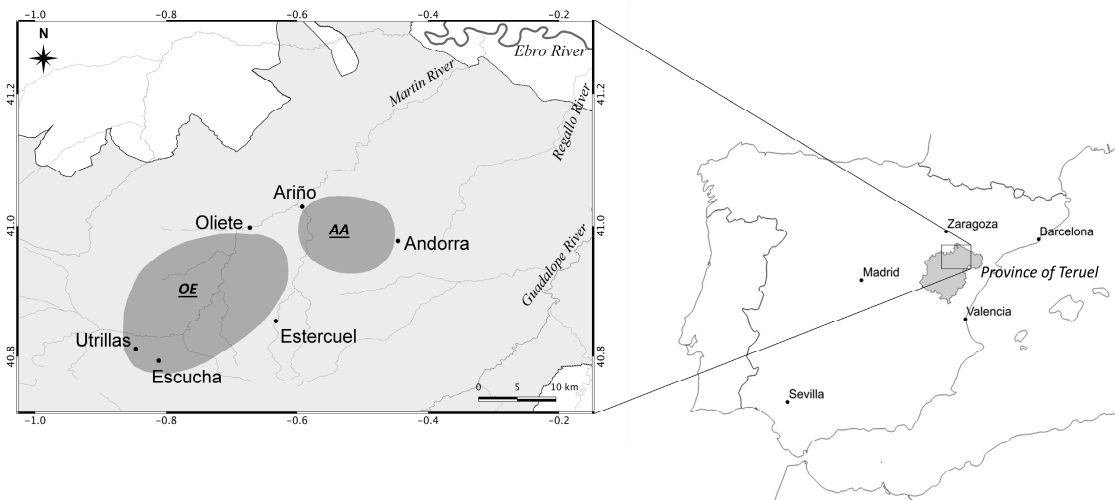


**Figure 1.** Location of the studied sampling areas. Legend: OE: Oliete-Estercuel; AA: Ariño-Andorra [3].

Mine spoils from the lignite mines associated with the Lignitos de Escucha (Escucha Lignites) and Arenas de Utrillas (Utrillas kaolinitic sands) formations belong to the upper part of the Lower Cretaceous [3]. These mine spoils have a great importance in the ceramic cluster of Castellón (Spain), due to their possibilities for being used as ceramic raw materials. These clayed mine spoils for industrial uses, on the basis on their mineralogy and chemical composition, can be classified as ball clays [1–3]. Some of these spoils are mined nowadays [4]. High-temperature mineral phases are generated in firing processes. Mineral phase transformations in a ceramic firing process have previously been described in literature [3,7]. Previously, a powerful study was carried out on the determination of high-temperature mineral phases using these mine spoils as ceramic raw material [3]. The formation of mullite and other high-temperature phases were studied in 2015 [3]. However, it was not possible to quantify the mineral phases and the vitreous phase present for each firing temperature. There is no information in the literature about the quantification of high-temperature phase generation and amorphous phase formation from these mine spoils for different firing temperatures. Knowledge and quantification of high-temperature minerals generated using these mine spoils as raw materials is interesting in industrial processes for manufacturing stoneware and ceramic tiles, as well as refractory ceramics [5–9]. In this work, for the first time, a quantification of mineral phase in the thermal transformations experienced by kaolinitic mine spoils has been carried out. The ceramic industry has been shown to have great potential to absorb industrial waste [8,9]. However, the commercial production of tiles from waste materials is very limited and, in some countries, non-existent. Some reasons include possible contamination by the waste used, the absence of relevant standards, and slow acceptance by industry and consumers. The main objectives of this paper are: (i) to understand the generation of high-temperature mineral phases after firing; (ii) to address a quantitative approach to minerals and amorphous phases present in ceramic tile bodies; (iii) to study the microstructure and porosity of ceramic tile bodies; and (iv) to contribute to a better knowledge of firing behavior of mine spoils, in order to promote their use in the Spanish ceramic industry as raw material in the manufacture of porcelain stoneware.

## 2. Materials and Methods

### 2.1. Mine Spoils

The geological background is described in [8]. The samples analyzed in this study were taken from a lignite mining area in the Iberian Range (Teruel, Spain). Sixty bulk samples of mine spoils were mineralogically and chemically analyzed, 40 of which came from the Oliete-Estercuel (OE) area, and 20 from the Ariño-Andorra (AA) mine area (Teruel, Spain). Ten representative samples from each area were selected, in order to separate them into three grain size fractions and, subsequently, carry out their mineralogical analysis. These fractions were separated from the bulk mine spoils following the standard protocols from ceramic industries. These mine spoils were classified as ball clays, and are mined today [1,3,4]. A representative sample of each deposit was selected for firing tests.

The mineralogical analysis was carried out using X-ray diffraction (XRD). The three fractions analyzed were: F1 (particle size  $<2\ \mu\text{m}$ ); F2 (particle size between 2 and  $50\ \mu\text{m}$ ); and F3 (particle size  $>50\ \mu\text{m}$ ). In the case of F1 and F2, oriented aggregates were prepared for the characterization of phyllosilicates, treated with ethylene glycol, and calcined at  $550\ ^\circ\text{C}$  for 2 h. XRD mineralogical quantitative approach was carried out (DIFFRACT.EVA and EDQ software v. 6.1.2, Bruker, Mannheim, Germany). The X-ray diffraction experiments were conducted in a Siemens D5000D powder diffractometer (Berlin, Germany) with the Bragg–Brentano  $\theta:2\theta$  configuration, using  $\text{Cu K}\alpha$  radiation (40 kV, 30 mA), aperture slit = 2 mm, divergence slit = 2 mm, detector slit = 0.2 mm, anti-scatter slit = 0.6 mm, and a graphite secondary monochromator. Samples were analyzed within the range of  $3\text{--}65^\circ$ . Measurements were taken at every  $0.04^\circ$  in a time step of 3.2 s. The X-ray diffraction plots were analyzed using Siemens automatic software for peak recognition, mineral identification, and peak intensity calculations.

The chemical analysis of the main elements was carried out by X-ray fluorescence (XRF) using conventional techniques, using a PHILIPS PW2400 X-ray Spectrometer (Mahwah, NJ, USA). Statistical correlations and cluster analysis were established, following the methodology described in [9].

### 2.2. Fired Samples

Four representative mine spoil samples from the OE area and two representative samples from the AA area were selected. From each selected sample, three replicas were prepared, following the protocol explained below. The selected clayed mine spoils (18 replicas) were moistened, mixed, and sieved (1 mm) until homogeneous agglomerates (6.5% of water) were made. They were pressed ( $300\ \text{kg}/\text{cm}^2$ ,  $80 \times 40 \times 5\ \text{mm}$ ) using a laboratory press (NANNETI mod. Mini-P, Faenza, Italy). The samples were fired to 995, 1050, 1100, and  $1150\ ^\circ\text{C}$ , keeping them for 4 h at the maximum firing temperature using a NANNETI kiln Mod. CVKN-CVKN/S, Faenza, Italy. A firing cycle similar to the one used in the local ceramic industry was simulated. A mineralogical analysis of the ceramic tile bodies (18 replicas  $\times$  4 temperatures) was carried out by XRD following the methodology described in [7–10], and by FTIR following the methodology described in [1]. In order to quantify mineral phase, ceramic pieces were ground in an agate hammer, homogeneously mixed with 10 wt% corundum, and analyzed by XRD, following the conventional RIRcor method [11]. Powder-fired samples were characterized by XRD techniques using a Siemens D5000D powder diffractometer with  $\text{Cu-K}\alpha$  radiation ( $\lambda = 1.5406\ \text{Å}$ ),  $2\theta$  in the interval between  $5$  to  $65^\circ$ , and a scanning rate of  $2^\circ/\text{min}$ . A method for crystalline and amorphous phase quantification was used. Once the majority of pure phases in the fired samples were identified, the corresponding calibration curves were built using 676-NIST (National Institute of Standards and Technology, Gaithersburg, MD, USA) as a reference. The RIRcor values of mullite, hematite, quartz, and hercynite were taken from [4]. For the FTIR analysis, a fine powder of the different ceramic tile bodies was placed on the glass window of the ATR-FTIR instrument spectrometer (BRUKER IFS 66/S, Mannheim, Germany). This device has a medium IR source, a KBr beamsplitter, and two detectors, including a DLaTGS detector (Mannheim, Germany) at room temperature for routine measurements and obtaining spectra between  $7000$  and  $400\ \text{cm}^{-1}$ . This method relies on the use of

the main band of a pure mineral as a reference for the normalization of the IR spectrum of a mineral sample. In this way, the molar absorptivity coefficient in the Lambert–Beer law and the components of a mixture, in mol percentage, can be calculated. GAMS equation modeling environment and the NLP solver CONOPT (©ARKI Consulting and Development, Bagsvaerd, Denmark) were used to correlate the experimental data in the samples considered. MCT (Mannheim, Germany) detector was cooled by high liquid nitrogen sensitivity and speed of measurement. Spectra were also compared to the RRUFF database (2237 Public Mineral Species with Samples, 3710 total Minerals Species with Samples): <https://rruff.info/>. This methodology allows the use of spectra libraries and linear regression algorithms for quantification purposes. A mercury penetrometer (POROSIZER 9329, Faenza, Italy) was used to determine some parameters that describe the porous texture of the studied ceramic tile bodies. Total volume of intrusion, the total pore area, the average pore radius, and apparent density of the test bodies were calculated from the intrusion curves for each of the fired tile bodies. Ceramic tile bodies were studied by back-scattering scanning electron microscopy (SEM) with energy dispersion microanalysis (EDS), using a PHILIPS XL-30 microscope (Mahwah, NJ, USA) with EDAX DX-4 microanalysis v.3.6 (0.3 mbar and 20 kV).

### 3. Results and Discussion

#### 3.1. Mine Spoils

The mineralogical composition of bulk materials was: quartz, feldspars, kaolinite, illite, chlorite and smectites (in traces), and minor hematite, calcite, and dolomite. Quantification of main minerals is shown in Table 1. The minerals detected in F1 were kaolinite and illite, sometimes they were also accompanied by chlorite.

**Table 1.** Mineralogical composition of mine spoils (bulk mine spoil). Mean value of the 60 samples analyzed, and range for each series (40 Oliete-Estercuel (OE) samples and 20 Ariño-Andorra (AA) samples).

Series (%)	Quartz		Kaolinite		Illite/Muscovite		Feldspars		Calcite/Dolomite	
	Mean	Range	Mean	Range	Mean	Range	Mean	Range	Mean	Range
OE	19.8	48–5	53.6	90–20	20.5	40–5	1.4	3–0	2.2	7–0
AA	40.3	59–17	35.8	49–17	19.6	50–8	0.9	6–0	-	-

The relative percentage of the main components for F1, illite and kaolinite, is recorded in Table 2. F2 has a similar composition to F1, but the kaolinite decreases and the illite content increases substantially (Figure 2). In F3, quartz is the main component and is always present, and illite/muscovite, dolomite, calcite, feldspars, and hematite can be present (Figure 2).

**Table 2.** Mineralogical composition of clay fractions (%kaolinite, %illite/muscovite). Mean value of the 60 samples analyzed, and ranges for each series (40 OE samples and 20 AA samples).

Series (%)	Kaolinite		Illite	
	Mean	Range	Mean	Range
OE	80.5	96–45	19.5	60–5
AA	65.3	80–39	34.7	65–21

Table 3 shows the chemical composition of the main components (mean and range) for each sampling area.

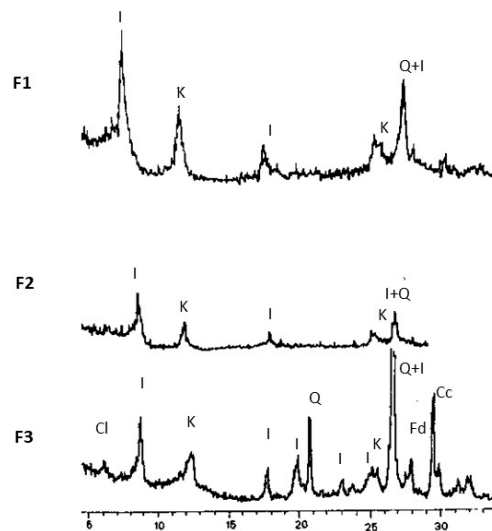


**Figure 2.** XRD diagrams for each particle size fraction: F1, F2, and F3 (from top to bottom, respectively). Legend: Q: quartz; I: Illite; K: kaolinite; Cl: chlorite; Fd: feldspar; Cc: calcite.

**Table 3.** Main elements (wt%). LOI: Loss on ignition.

Series	SiO <sub>2</sub>		Al <sub>2</sub> O <sub>3</sub>		CaO		MgO		K <sub>2</sub> O		Fe <sub>2</sub> O <sub>3</sub>		LOI	
	Mean	Range	Mean	Range	Mean	Range	Mean	Range	Mean	Range	Mean	Range	Mean	Range
OE	55.5	64–41	25.7	33–19	0.72	3.0–0.2	0.70	1.8–0.4	1.92	3.5–0.6	4.38	8.2–1.3	15.8	17.2–6.2
AA	64.6	70–58	20.71	24–13	0.41	0.6–0.2	0.41	0.6–0.2	2.09	3.8–0.1	3.12	4.5–1.3	8.59	10–4.8

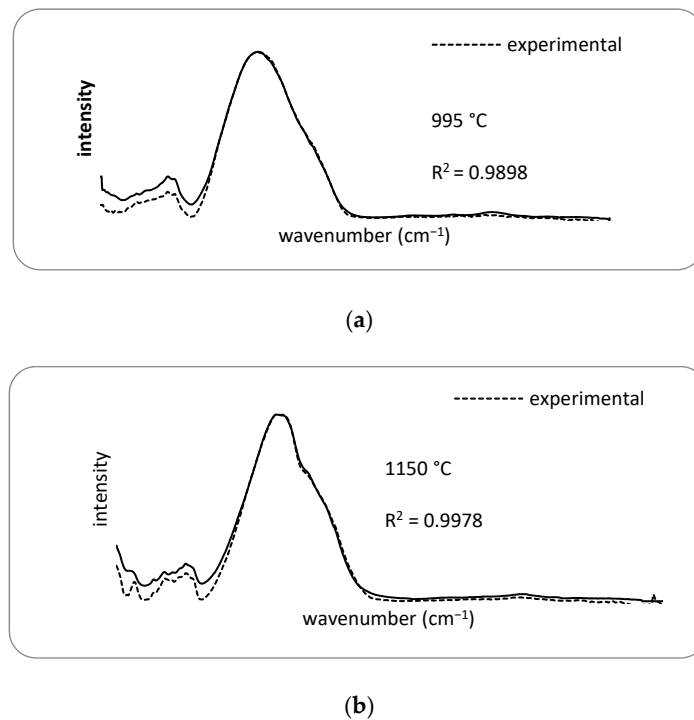
### 3.2. Fired Bodies

Table 4 show the mineral quantification of analyzed fired bodies for each temperature. All analyzed samples contain a high percentage of kaolinite and illite. The presence of micaceous minerals along with kaolinite is quite common in many ceramic clays [12]. This is the case for all the analyzed samples that contain illite. Therefore, in this section, we consider the firing transformations experienced by clayed mine spoils. In other words, the formation of mullite and other high-temperature phases were studied from mine spoils that have variable proportions of illite (between 4% and 50%) and/or chlorite (<5%). Cristobalite was not detected as a high-temperature phase in either of the series (OE or AA). Table 4 summarizes the aforementioned results regarding the observations made with FTIR (Figure 3) and XRD (Figure 4).

**Table 4.** Mineral quantification of fired tile bodies (%).

T (°C)/Mineral Phase (%)	Mullite	Quartz	Hematite	Spinel/Hercynite	Vitreous Phase
Serie OE					
995	18	15	5	5	57
1050	23	10	7	4	56
1100	28	6	9	3	54
1150	39	2	12	1	46
Serie AA					
995	8	21	9	7	55
1050	11	11	7	5	66
1100	17	8	12	3	60
1150	28	4	19	2	47

S.D ± 1.



**Figure 3.** FTIR experimental spectra for fired sample bodies and their calculated FTIR spectra. Temperatures: 995 °C (a) and 1150 °C (b).

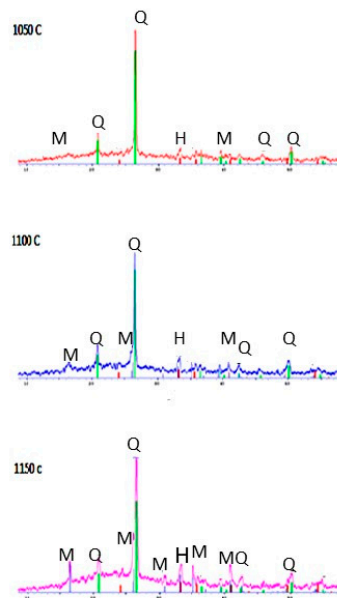


**Figure 4.** XRD diagrams of test bodies heated at different temperatures. Legend: Q: quartz; H: hematite; M: mullite.

More or less significant amounts of amorphous material and glassy phase were detected in all fired samples. According to the literature [13,14], there is no interaction between the kaolinite and illite particles of clays fired under 1000 °C. Mullite formation after high-temperature illite breakdown has been studied in phyllosilicate-rich bricks [15]. At  $T \geq 900$  °C, illite dehydroxylation is followed by partial melting that triggers the nucleation and growth of mullite [15]. This absence of interaction would be the cause behind the temperature of formation of the spinel phase being separate from the illite content. Therefore, the mullitization process can be explained independently. The creation of

mullite from illite at a lower temperature [15] than the one that leads to the transformation of kaolinite can be attributed to the effect of potassium and other alkaline or alkaline-earth cations present in (or near) the porous hexagonal network of the tetrahedral sheets (containing Si) in 2:1 layers of illite. The effect of K in these positions is similar to the role conducted by this element in glass formation. As the Si–O bonds break, the potassium ions move, keeping the structure open and not allowing atoms to bond back together. As a result, the stability of the tetrahedral layer is significantly reduced compared to its normal stability, which facilitates the structural transformation into mullite at a low temperature. Potassium, therefore, decreases the activation energy required to create mullite. The relative amount of alumina present in illite that is available for the formation of mullite at high temperatures is lower than in kaolinite. As a result, in mine spoils with a high proportion of illite/kaolinite, the amount of mullite that can be created in the fired tile bodies is considerably smaller than in pure kaolinite. The non-existence of cristobalite in clays that are rich in illite can be explained by taking into consideration the chemical composition of illite.

By increasing the content in illite, when going from pure kaolinites to mixtures and pure illite, the amount of silica available for the formation of cristobalite also increases slightly, but the content of alkaline metals that create glass increases much more. As a result, the absence of cristobalite is attributed to the presence of glass-forming cations supplied by the illite.

At 995 °C, the formation of a noticeable amount of mullite can be attributed to the high content of illite. Even so, lengthy firing times are needed to be able to observe clearly-defined reflections of mullite in the diffractogram.

At 1050 °C, the 55 °C rise in firing temperature causes an increase in the percentage of mullite in both samples, and the formation of mullite is much more intense. These samples show the most intense and closest reflections. At 1100 °C, we obtained diffractograms with very intense and well-defined lines of mullite (Figure 4). At 1150 °C, the development of mullite is clear in all samples, and with high crystallinity.

According to the quantification XRD analyses (Table 4), mullite is the most abundant mineral. The hercynite content is higher at low temperatures (995 °C), and hematite content is higher at 1150 °C. The highest quartz content is slightly over 20% in samples from the AA mine area. Compared to the other crystalline phases present in the fired samples, an intermediate phase between spinel ( $\text{MgO}\cdot\text{Al}_2\text{O}_3$ ) and hercynite ( $\text{FeO}\cdot\text{Al}_2\text{O}_3$ ) is originated from the destruction of illite [10]. In the samples richer in illite, hercynite forms directly [10]. This phase is formed at 995 °C and remains up to a temperature of 1150 °C. Firstly, at 995–1100 °C, a great change in the structure takes place and a spinel phase is formed. The crystallinity of spinel and glassy phases are evolved in a wide temperature range between 995 and 1150 °C.

Along with the incongruent fusion of the feldspars, the formation of the vitreous phase and the final mullitization were observed (Figure 5). Between 1050 and 1100 °C there is an important decrease in the open porosity in AA fired samples, coinciding with the first phase of vitrification (Table 5). This behavior is not observed in the OE fired samples, where the open porosity increases between 1050 and 1100 °C. This behavior is probably due to the higher mullite content of the OE fired samples at these temperatures. At 1150 °C, both fired samples OE and AA close their pores, and the porosity decreases significantly [7,10]. An Al- and Si-rich vitreous phase is formed by the decomposition of the initial minerals due to the increase in temperature, and it represents about 50% of the fired bodies. The higher percentages in mullite and vitreous phases at 995 °C is explained by the presence of an abundance of illite in all samples [15].

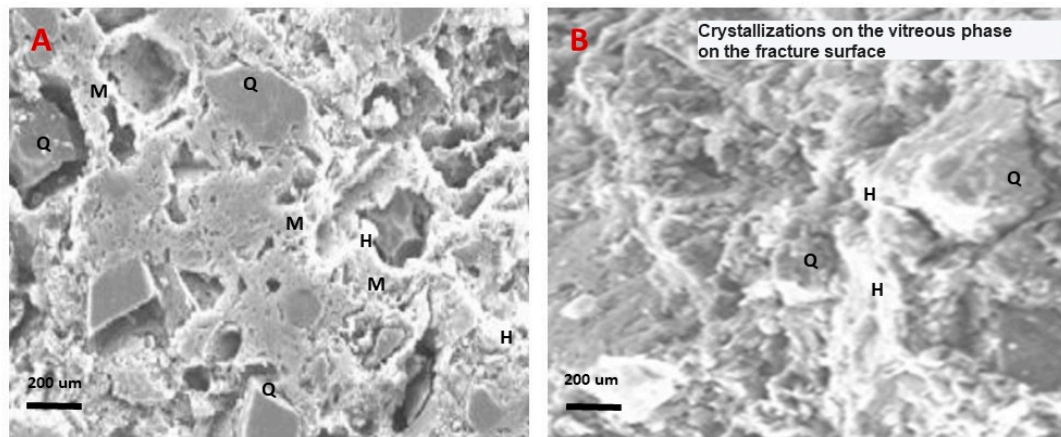


**Figure 5.** Growth of minerals, and presence of abundant vitreous phase and low porosity in tile bodies fired at 1150 °C. (A) The presence of quartz and amorphous phase were observed together with small scale-shaped crystals of type I primary mullite (<0.2 µm in size). (B) Crystallizations on the vitreous phase on the fracture surface. Hematite coatings are observed forming crusts.

**Table 5.** Parameters that describe the porous texture of the ceramic tile bodies.

Sample	T (°C)	VT (mL/g)	ST (m <sup>2</sup> /g)	$\varphi$ (g/mL)	$\varphi_{ap}$ (g/mL)	$\epsilon$	Kp.10–16 (m)	r.10–8 (m)
OE	995	0.142	2.09	1.895	2.603	0.375	8.72	13.44
	1050	0.074	1.78	2.186	2.577	0.180	1.59	8.22
	1100	0.135	2.29	1.944	2.601	0.344	6.01	11.97
	1150	0.030	1.684	2.243	2.480	0.083	0.06	5.98
AA	995	0.143	3.505	1.919	2.668	0.285	2.43	8.40
	1050	0.100	1.917	2.125	2.696	0.222	3.25	10.40
	1100	0.061	1.345	2.286	2.620	0.142	1.32	8.86
	1150	0.038	1.745	2.352	2.581	0.092	0.25	4.33

Legend: T (temperature); VT (total Hg volume that penetrates into the pores); ST (specific surface);  $\varphi$  (density);  $\varphi_{ap}$  (apparent density);  $\epsilon$  (open porosity); Kp (coefficient of permeability); r (average pore radius).

The presence of quartz and amorphous phase were observed by SEM, together with small scale-shaped crystals of type I primary mullite. Also, hematite coatings were observed forming crusts. Most of the small quartz (<25 µm) is included in the vitreous matrix. Despite observing a porous microstructure, the non-porous areas are well sintered.

#### 4. Conclusions

Mine spoils with a high amount of illite create mullite at 995 °C. Cristobalite was not detected as a high-temperature phase. More or less significant amounts of amorphous material and glassy phase were detected in all fired samples (>45%). The higher percentages of mullite (18–8%) and vitreous phase (>55%) at 995 °C were due to the presence of an abundant amount of illite in all samples. At 1150 °C, the content of mullite in the fired OE selected samples (39%) was higher than the ones from the AA series (28%). Between 1050 and 1100 °C, there is an important decrease in the open porosity in AA fired samples. However, this behavior is not observed in the OE fired samples, where the open porosity increased between 1050 and 1100 °C. The role of the mullite in this behavior could be an area for future new research. Despite observing a porous microstructure, the non-porous areas are well sintered. The presence of quartz and amorphous phase were observed together with small scale-shaped crystals of mullite and hematite coatings forming crusts.

**Author Contributions:** Conceptualization, M.M.J. and S.M.; methodology, M.M.J. and S.M.; software, S.M.; validation, S.M., F.P. and M.A.M.; formal analysis, S.M. and M.M.J.; investigation, M.M.J., S.M., M.A.M. and F.P.; writing—original draft preparation, M.M.J.; writing—review and editing, M.M.J.; supervision, M.M.J.; project administration, M.M.J. All authors have read and agreed to the published version of the manuscript.

**Funding:** This research received no external funding.

**Acknowledgments:** The authors would like to express their gratitude to Emilio Galán for his help in the discussion and comments; and dedicate this manuscript to the memory of T. Sanfeliu, for his hard work in the study of Spanish ceramic clays.

**Conflicts of Interest:** The authors declare no conflict of interest.

## References

1. Jordá, J.D.; Vidal, M.M.J.; Ibanco-Cañete, R.; Montero, M.; Labarta, J.A.; Sanchez, A.S.; Cerdán, M. Mineralogical analysis of ceramic tiles by FTIR: A quantitative attempt. *Appl. Clay Sci.* **2015**, *115*, 1–8. [[CrossRef](#)]
2. Dondi, M.; Raimondo, M.; Zanelli, C. Clays and bodies for ceramic tiles: Reappraisal and technological classification. *Appl. Clay Sci.* **2014**, *96*, 91–109. [[CrossRef](#)]
3. Vidal, M.M.J.; Meseguer, S.; Pardo, F.; Montero, M. Properties and possible ceramic uses of clays from lignite mine spoils of NW Spain. *Appl. Clay Sci.* **2015**, *118*, 158–161. [[CrossRef](#)]
4. Laita, E.; Bauluz, B.; Yuste, A. High-Temperature Mineral Phases Generated in Natural Clinkers by Spontaneous Combustion of Coal. *Minerals* **2019**, *9*, 213. [[CrossRef](#)]
5. Bauluz, B.; Mayayo, M.J.; Yuste, A.; Fernández-Nieto, C.; López, J.M.G. TEM study of mineral transformations in fired carbonated clays: Relevance to brick making. *Clay Miner.* **2004**, *39*, 333–344. [[CrossRef](#)]
6. Bastida, J.; Lores, M.T.; De la Torre, J.; Pardo, P.; Buendia, Y.A.M.L. Microstructural modification of Clay minerals in ball clays from Teruel by thermal treatment. *Bol. Soc. Esp. Cerám. Vidr.* **2006**, *49*, 38–45.
7. Vidal, M.M.J.; Montero, M.; Meseguer, S.; Sanfeliu, T. Influence of firing temperature and mineralogical composition on bending strength and porosity of ceramic tile bodies. *Appl. Clay Sci.* **2008**, *42*, 266–271. [[CrossRef](#)]
8. Meseguer, S.; Vidal, M.M.J.; Sanfeliu, T. Use of mine spoils from Teruel coal mining district (NE, Spain). *Environ. Earth Sci.* **2008**, *56*, 845–853. [[CrossRef](#)]
9. Meseguer, S.; Sanfeliu, T.; Vidal, M.M.J. Classification and statistical analysis of mine spoils chemical composition from Oliete basin (Teruel, NE Spain). *Environ. Earth Sci.* **2008**, *56*, 1461–1466. [[CrossRef](#)]
10. Jordán, M.; Boix, A.; Sanfeliu, T.; De La Fuente, C. Firing transformations of cretaceous clays used in the manufacturing of ceramic tiles. *Appl. Clay Sci.* **1999**, *14*, 225–234. [[CrossRef](#)]
11. Hillier, S. Quantitative analysis of clays and other minerals in sandstones by X-ray power diffraction (XRPD). *Int. Assoc. Sedimentol. Publ.* **2003**, *34*, 213–251.
12. Laita, E.; Bauluz, B. Mineral and textural transformations in aluminium-rich clays during ceramic firing. *Appl. Clay Sci.* **2018**, *152*, 284–294. [[CrossRef](#)]
13. Ferrari, S.; Gualtieri, M.L. The use of illitic clays in the production of stoneware tile ceramics. *Appl. Clay Sci.* **2006**, *32*, 73–81. [[CrossRef](#)]
14. Sanfeliu, T.; Vidal, M.M.J. Geological and environmental management of ceramic clay quarries: A review. *Environ. Earth Sci.* **2008**, *57*, 1613–1618. [[CrossRef](#)]
15. Rodríguez-Navarro, C.; Cultrone, G.; Navas, A.S.; Sebastian, E. TEM study of mullite growth after muscovite breakdown. *Am. Mineral.* **2003**, *88*, 713–724. [[CrossRef](#)]



© 2020 by the authors. Licensee MDPI, Basel, Switzerland. This article is an open access article distributed under the terms and conditions of the Creative Commons Attribution (CC BY) license (<http://creativecommons.org/licenses/by/4.0/>).